AUTOMATIC DETECTION AND SEGMENTATION OF BREAST LESIONS ON MR IMAGES USING 3D LEVEL SET TECHNIQUE

F. Veronesi[*,**], C. Corsi[*], A. Sarti[*], L. Bocchi[***] and C. Lamberti[*]

[*]DEIS, University of Bologna, Bologna, Italy
[**]Polytechnic of Milan , Milan, Italy
[***]University of Florence , Florence, Italy

fveronesi@deis.unibo.it

Abstract: Magnetic Resonance Imaging (MRI) is an often used imaging technique for the detection of breast cancer. This imaging technique offers the possibility to acquire three-dimensional data set and to highlight the tissues that have a characteristic pathological behaviour by using a contrast medium agent. We propose a method to overcome the time consuming operation needed to analyze these types of dataset. By using a region based level set algorithm we segment in the 3D space the regions of the images that have a time-enhancement curve compatible with the presence of a malignant lesion. By using this segmentation technique it is also possible to get volumetric information such as spatial position, mass volume and shape. The analysis performed on 12 unselected patients showed good results, all the lesions were detected and correctly segmented. In conclusion we propose a fast, automatic and accurate method for the detection and the segmentation of breast lesion in three-dimensional breast MR dataset.

Introduction

Breast cancer is by far the most frequent cancer in women (23% of all cancer with 1.15 million new cases in 2002 [1]) but thanks to the screening program precocious diagnosis is possible and so this pathology shows high survival rate (73%, in developed countries).

X-ray mammography is the imaging technique most commonly used to perform breast cancer screening and offers the possibility to get images representative of the density of breast tissues [2]. There are two major problems with this technique:

1. the resulting images are 2D projection of a 3D structure, thus it is not possible to precisely localize the suspected lesion and estimate its dimension;
2. the presence of dense tissues (especially in young women), scar tissue or an hormone therapy in act can alter the efficiency of mammography exam. In fact, in these cases the simple analysis of the density of tissue is not sufficient and a more detailed analysis is needed.

Magnetic Resonance Imaging (MRI) offers the possibility to solve these problems, since current MRI equipment allows 3D acquisitions with spatial resolution up to 0.5mm in the slices and up to 2-3mm between slices (slice thickness). Higher luminosity on the image in correspondence of major blood presence is obtained by the injection of contrast enhancement agent into patient blood. It is proved that malignant lesions release angiogenic factors that produce a growth of capillary and the formation of new vessels [3, 4]. By highlighting on the image the high vessel density of the lesions, the use of contrast enhancement agent improves the possibility to distinguish different tissues and lesions. Moreover no ionizing rays, that are harmful for patients, are used. However MRI spatial resolution is lower and the exam is longer and more expensive than mammography; moreover the refertation is time consuming. In clinical practice nowadays MRI is often used as second step exam, especially in case of suspicious or uncertain masses, because it gives more information about the nature of the lesion. Nevertheless the evaluation of MRI data, as it is presently done, is limited to the visual evaluation of the enhancement-time curves of suspicious Region Of Interest (ROI). The ROI is usually a fixed 2D region that clinician arbitrary chooses among the subtracted (after-contrast minus pre-contrast image) slices; the enhancement curve of this ROI is plotted and visually evaluated accordingly to the category showed in Figure 1 [4, 5]. Once a suspicious region is detected it is measured the maximum length of the detected mass. The limitations of this clinical protocol are evident: it is time consuming, there is high intra-observer variability and it is limited to bi-dimensional analysis.

In this paper we propose a semi-automatic technique to detect and segment breast lesions in 3D space.

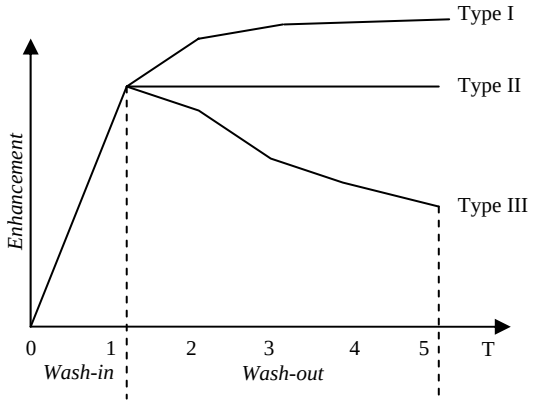

Figure 1: Plot of the possible time-enhancement curves of the tissues in MRI using contrast agent. Type III denotes the presence of a suspicious lesion.

ISSN: 1727-1983

Materials and Methods

To acquire data from 12 unselected patients we used a 1.5 T MR applying the 3D FFE (Fast Field Echo) sequence, five or six datasets of the whole volume were acquired, one before and the others after the injection of 0.2 mmol/Kg of Gd-DTPA. The acquisition was on coronal plane and included both breasts simultaneously (bilateral acquisition).

The basic goal of level set techniques is to evolve a surface in order to detect objects in an image starting from an initial condition. We used a modified region-based level set [6] approach for the 3D space in order to isolate regions that have similar pathologic enhancement curve. To detect suspicious regions we don't analyze subtracted images, as is usual in clinical practice [4, 5], but we analyze automatically and simultaneously the 5-6 datasets acquired for each patients. During the evolution of level set we minimize a functional that takes account of the variation of intensity of each voxel during time. In fact, the functional is dependent by the area under the time-enhancement curve of the voxels.

The Chan-Vese [6] method for segmenting images is based on the identification of the region that minimizes an energy function. Let us define the evolving curve C in Ω, as the boundary of an open subset ω of Ω (i.e. $\omega \subset \Omega$, and $C = \partial\omega$). The region we want to segment is ω and correspond to $inside(C)$ and the region $outside(C)$ is $\Omega \setminus \omega$. The basic idea of this model can be explained by using a simple example of an image u_0 that contains only two values: u_0^i is the value of the inside region, to be segmented, and u_0^o is the outside value. Let us consider the term:

$$F_1(C) + F_2(C) = \int_{inside(C)} |u_0(x,y) - c_1|^2 \, dx\, dy + \int_{outside(C)} |u_0(x,y) - c_2|^2 \, dx\, dy \tag{1}$$

where C is any other variable curve, and the constants c_1 , c_2 , depending on C , are the averages of u_0 inside C and respectively outside C . In this simple case C_0 , the closed boundary of the object, is the minimizer of this term:

$$\inf_C \{F_1(C) + F_2(C)\} \approx 0 \approx F_1(C_0) + F_2(C_0) \, . \tag{2}$$

It is possible to see that if the curve C is outside the region to be segmented then $F_1(C) > 0$ and $F_2(C) \approx 0$ (fig. 2A); if it is completely inside $F_1(C) \approx 0$ and $F_2(C) > 0$ (fig. 2B); if the curve is both inside and outside the region then $F_1(C) > 0$ and $F_2(C) > 0$ (fig. 2C). Only if the curve is on the boundary of the region, $C \equiv C_0$, then $F_1(C) \approx F_2(C) \approx 0$ (fig. 2D).

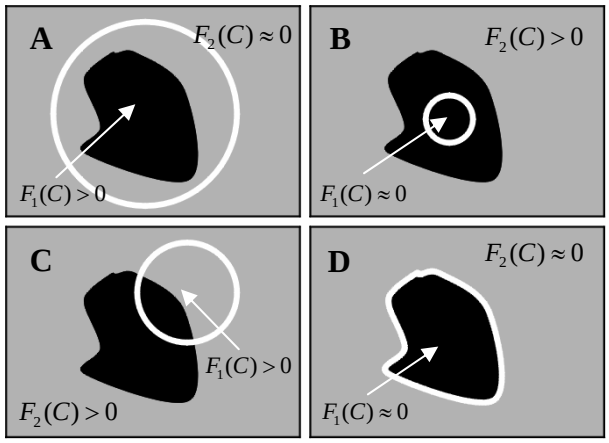

Figure 2: Evaluation of the terms of equation (1) in a simple case in which the image contains only two uniform region: the black one to be segmented and the gray one.

In addition to the terms of (1) two terms of regularization were added in the Chan-Vese model, one relative to the length of C and one relative to the area inside C . By introducing the energy functional $F_1(c_1, c_2, C)$ and the regularization terms the equation (1) becomes:

$$\begin{aligned} F(c_1, c_2, C) = {} & \mu \cdot Length(C) + \nu \cdot Area(inside(C)) \\ & + \lambda_1 \int_{inside(C)} |u_0(x,y) - c_1|^2 dx\, dy \\ & + \lambda_2 \int_{outside(C)} |u_0(x,y) - c_2|^2 dx\, dy, \end{aligned} \tag{3}$$

where $\mu \geq 0,\ \nu \geq 0,\ \lambda_1, \lambda_2 > 0$ are fixed parameters. Therefore the problem considered is the minimization of:

$$\inf_C F(c_1, c_2, C) \, . \tag{4}$$

The dataset we want to analyze are three-dimensional and time dependent (5 or 6 acquisition at different time). In our active contour model the Chan-Vese model is modified for the 3D space and moreover the terms $F_1(C)$ and $F_2(C)$ are substitued with functions that consider not only the value of the point into the image but also the variation of the brightness during the time. In what follows the boundary C of the region to be segmented is a surface, the parameters are $\lambda_1 = \lambda_2 = 1$ and $\nu = 0$ so that the area (volume) regularization term is omitted. Therefore the equation (3) in our model becomes:

$$\begin{aligned} F(c_1, c_2, C) = {} & \mu \cdot Surface(C) \\ & + \int_{inside(C)} \left| \left(\sum_{i=0}^{n} u_i(x,y,z) \right) - c_1 \right|^2 dx\, dy\, dz \\ & + \int_{outside(C)} \left| \left(\sum_{i=0}^{n} u_i(x,y,z) \right) - c_2 \right|^2 dx\, dy\, dz \end{aligned} \tag{5}$$

ISSN: 1727-1983

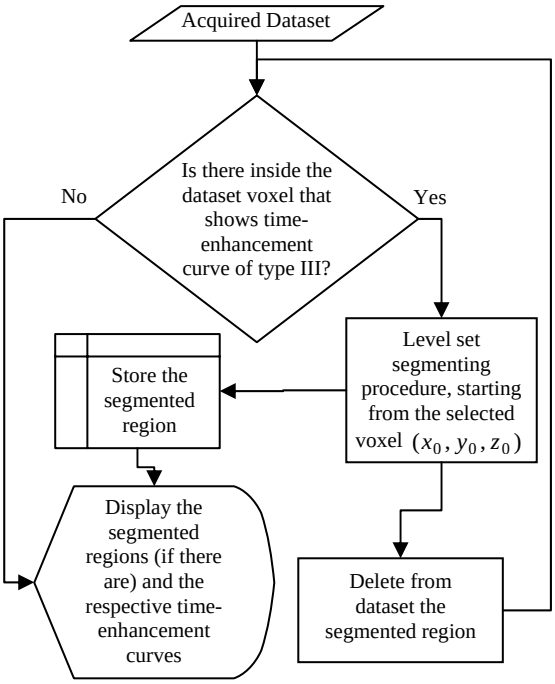

Figure 3: Flow chart of the sequence of action automatically done by the procedure for suspicious mass detection.

where $i = 0...n$ is relative to the istant of the dataset acquisition; $i = 0$ is the istant of the anatomical acquisition in which the contrast agent in not yet injected.

By applying to this problem the level set method proposed by Osher-Sethian [7] the boundary $C \subset \Omega$ is represented by the zero level set of a Lipschitz function $\phi : \Omega \to \mathbb{R}$, such that:

$$\begin{cases} C = \delta\omega = \{(x, y, z) \in \Omega : \phi(x, y, z) = 0\} \\ inside(C) = \omega = \{(x, y, z) \in \Omega : \phi(x, y, z) > 0\} \\ outside(C) = \Omega \setminus \omega = \{(x, y, z) \in \Omega : \phi(x, y, z) < 0\} \end{cases} \quad (6)$$

And thus

$$C = \phi^{-1}(0).$$

By using the Heaviside function is possible to evaluate the integral inside and outside a function ϕ in the space Ω. Let us define also the delta of Dirac function as the first derivative of the Heaviside function:

$$H(\phi) = \begin{cases} 1, & \text{if } \phi \geq 0 \\ 0, & \text{if } \phi < 0 \end{cases}, \quad \delta_0(\phi) = \frac{d}{d\phi} H(\phi). \quad (7)$$

The terms of the energy function (5) can now be written as:

$$\begin{aligned} F(c_1, c_2, \phi) &= \mu \cdot \int_\Omega \delta_0(\phi(x, y, z)) |\nabla \phi(x, y, z)| \, dx\, dy\, dz \\ &+ \int_\Omega \left| \left(\sum_{i=0}^{n} u_i(x, y, z) \right) - c_1 \right|^2 H(\phi(x, y, z))\, dx\, dy\, dz \\ &+ \int_\Omega \left| \left(\sum_{i=0}^{n} u_i(x, y, z) \right) - c_2 \right|^2 (1 - H(\phi(x, y, z)))\, dx\, dy\, dz \end{aligned} \quad (8)$$

The constant c_1, c_2 are rapresentative of the average inside and outside the zero level set surface of ϕ and can be expressed as:

$$\begin{aligned} c_1(\phi) &= \frac{\int_\Omega \left(\sum_{i=0}^{n} u_i(x, y, z) \right) H(\phi(x, y, z))\, dx\, dy\, dz}{\int_\Omega H(\phi(x, y, z))\, dx\, dy\, dz} \quad \text{and} \\ c_2(\phi) &= \frac{\int_\Omega \left(\sum_{i=0}^{n} u_i(x, y, z) \right) (1 - H(\phi(x, y, z)))\, dx\, dy\, dz}{\int_\Omega (1 - H(\phi(x, y, z)))\, dx\, dy\, dz}. \end{aligned} \quad (9)$$

Now let us adding an auxiliary time variable (different from the sequence time *i*) to the level set function $\phi(x, y, z)$, so that $\phi(x, y, z, t) : \Omega \times [0, T[\to \mathbb{R}$. In this way the evolution of the surface C at time t can be expressed by the zero level set:

$$C(t) = \phi(t)^{-1}(0). \quad (10)$$

The solution of the problem can be obtained by minimizing the energy function (8); keeping c_1, c_2 fixed with respect to ϕ it is possible to identify the steepest descent, the Euler-Lagrange equation:

$$\begin{cases} \dfrac{\partial \phi}{\partial t} = 0 = \delta(\phi) \left[\mu \, \mathrm{div}\left(\dfrac{\nabla \phi}{|\nabla \phi|} \right) - \left| \left(\sum_{i=0}^{n} u_i(x, y, z) \right) - c_1 \right|^2 \right. \\ \qquad \left. + \left| \left(\sum_{i=0}^{n} u_i(x, y, z) \right) - c_2 \right|^2 \right] \qquad \text{in } \Omega \times]0, \infty[\\ \phi(x, y, z, 0) = \phi_0(x, y, z) \qquad \text{in } \Omega \\ \dfrac{\partial(\phi)}{|\nabla \phi|} \dfrac{\partial \phi}{\partial \vec{n}} = 0 \qquad \text{on } \partial\Omega \end{cases} \quad (11)$$

where $\vec{n}$ is the exterior normal to the boundary $\partial\Omega$. The first term on the right hand side denotes the Euclidean curvature. The second equation represents the initial condition. The third equation is the boundary condition. As initial condition we use a distance function defined as:

$$\phi_0(x, y, x) = \sqrt{(x - x_0)^2 + (y - y_0)^2 + (z - z_0)^2} - R, \quad (12)$$

where R is the radius of the starting sphere. To determine the center of this sphere, that is the starting point of the evolution, we choose the voxels of the dataset that show time-enhancement curve compatible with the characteristic curve of lesions. The characteristic time-enhancement curve has these features [4, 5]:

- high signal intensity (SI) enhancement rate after contras agent injection: $\lfloor (SI_{post} - SI_{pre}) / SI_{pre} \rfloor \cdot 100$;
- rapid initial enhancement (*wash-in*): maximum enhancement in the first (*i*=1) or second (*i*=2) dataset acquisition after contrast medium injection ;
- rapid decrease of the enhancement (*wash-out*) in the final datasets acquisitions (*i*=3,4,5).

ISSN: 1727-1983

Table 1: Summary of the result of the computation compared with Medical Doctor Report for the 12 studied patients. (RB=Right Breast or LB=Left Breast, S=Superior or I=Inferior, E=Exterior or I=Interior)

	Medical Doctor Report			**Automatic Software Analysis**				
Patient	**Number of lesions**	**Position of lesion**	**Dimension (mm)**	**Number of lesions**	**Position of lesion**	**Dimension (mm^3) (mean linear dimension (mm))**	**Computation time (s)**	**False positive**
Pt. #1	4	RB, SE RB, II RB, II Armpit	15 5 5 30	6	RB-SE RB-II RB-II Armpit	661 (15.8) 116 (8.9) 112 (8.9) 1836 (22.3)	160	2
Pt. #2	1	RB, II	6	1	RB-II	47 (6.6)	25	0
Pt. #3	1	RB, IE	10	4	RB, IE	2903 (25.8)	285	3
Pt. #4	1	LB, SE	12	1	LB, SE	183 (10.3)	20	0
Pt. #5	1	RB, II	8	1	RB, II	182 (10.3)	20	0
Pt. #6	1	LB, II IE	19	2	LB, II IE	2366 (24.2)	75	1
Pt. #7	2	RB, II LB, SI	17 10	3	RB, II LB, SI	1790 (22.1) 1493 (20.8)	135	1
Pt. #8	1	LB, E	8	1	LB, E	107 (8.6)	80	0
Pt. #9	1	LB, II	28	2	LB, II	1375 (20.2)	60	1
Pt. #10	1	LB, S	10	3	LB, S	415 (13.6)	75	2
Pt. #11	1	LB, SI SE	10	1	LB, SI SE	368 (13.0)	85	0
Pt. #12	1	RB	wide	2	RB	1790 (22.1)	130	1

These features are characteristic of the time-enhancement curve of type III (figure 1).

After the detection of the voxel that better approximate the curve features of a suspicious lesion, the level set segmentation algorithm is applied in order to detect the region in which the voxels have similar and homogeneous time-enhancement curve. This detected region is then deleted from dataset and it is searched inside the dataset another voxel that has the curve features of suspicious mass in order to detect multi-focal lesions. This loop, that the procedure automatically computes, is showed in the flow chart of figure 3. Only if all the regions considered suspicious are segmented (if they are present) the results are displayed on the screen.

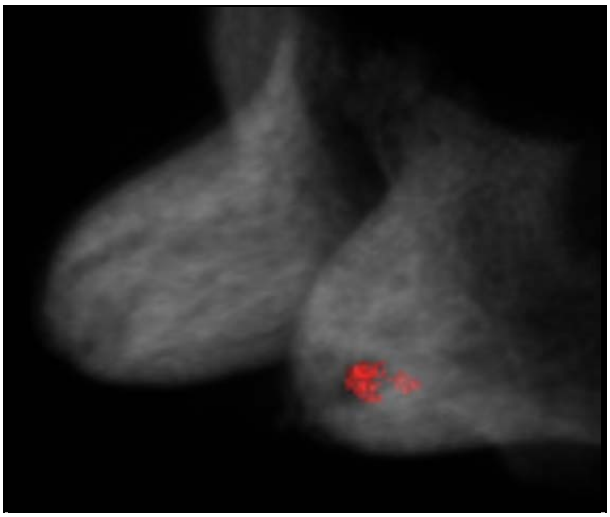

Figure 4: Volume rendering of the dataset generated from the procedure in which the mass is highlighted.

After this it is generated a dataset in which the detected masses are highlighted; this data can be displayed in a three-dimensional volume rendering visualization (figure 4) for the spatial localization and the mass shape analysis.

At the end of the automatic analysis of the dataset all the segmented regions are shown at display with three orthogonal views and the plot of the mean time-enhancement curve (figure 5). From these visualizations the operator can classify the detected region as pathological or a false positive detection and then compute the mass volume.

Results

The computations were performed using MatLab 7.0 on a Pentium IV, 2.6 GHz, 1Gb RAM. The results of the automatic analysis were compared with the report produced by the manual analysis of expert medical doctor; in table 1 is showed the summary of the obtained results. The computation time ranged between 25 seconds and 285 seconds while the manual analysis requires 10-20 minutes depending on the experience of the operator. The parameter is set to 1 and the radius of the distance function is R=2.

All the lesions (16/16) were detected with no false negative. The automatic analysis detected 11 false positive that showed suspicious time-enhancement curves. The position of the detected masses is correspondent between the two analyses even if the automatic analysis could give as output the spatial

ISSN: 1727-1983

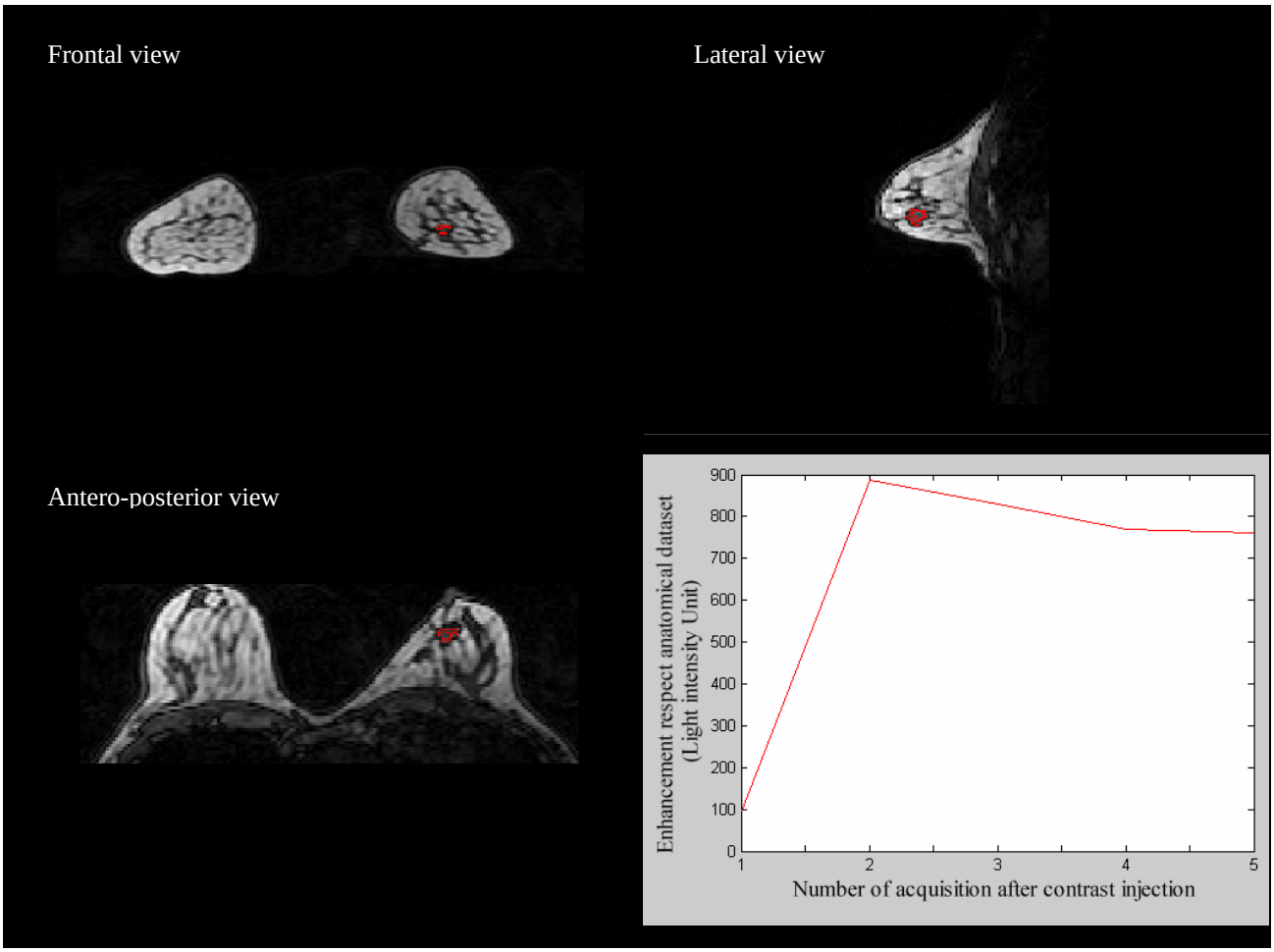

Figure 5: Visualization of the result of the segmentation procedure and the volume rendering of the modified dataset.

coordinate triplet (x,y,z) corresponding to the center of the lesion for precise localization. The dimensions of the lesions for the clinical report are expressed with a length in millimeters. Using the computer aided analysis the dimensions are evaluated in mm3 because they refer to a volumetric quantification. In order to allow a qualitative comparison between these two values the mean linear dimension of the lesion is presented inside the brackets.

Discussion

The method we propose for the analysis of breast MRI exams can automatically detect and segment suspicious mass. In fact all the lesions that the clinician found were detected in the same position. The presence of false positive results is due to the presence of region that shows the same time-enhancement as the detected masses. In fact, motion artifact and vessels presence sometime can show a curve of type III, but when a clinician check the displayed images can easily distinguish this kind of region from the pathological ones. The possibility to get volumetric information about the lesion instead of its major linear dimension allows clinician to better characterize the mass analyzing its extension and its shape. The time required for the whole dataset analysis is significantly inferior in the computer aided analysis; moreover during this kind of analysis the clinician intervention is required only at the end of the procedure. At this moment the operator has to identify where segmented regions are lesions or artifacts. The position of the mass, by using our method, can be easily found. This information combined with the possibility to visualize the volume in a virtual 3D space allows clinicians to get important information about the localization of the mass. This information could be very useful during the biopsy and in planning a surgery intervention.

Conclusions

We presented a method that can automatically analyze an MRI breasts dataset in order to detect suspicious masses by using a level set algorithm. Our method is fast and accurate; moreover it gives the possibility to get volumetric information about position, dimensions and shape that can allow accurate diagnosis.

Acknowledgements

The authors thank Sandro Quaranta, MD, Gioele Santucci, MS and Marcella Zangheri, MS of the AUSL of Rimini for they invaluable contribution.

ISSN: 1727-1983

References

[1] PARKIN, D.M., BRAY, F., FERLAY, J., PISANI, P. (2005): 'Global Cancer Statistics, 2002', CA Cancer J Clin, **55,** pp. 74-108

[2] SICKLES, E.A., MIGLIORETTI, D.L., BALLARD-BARBASH, R., GELLER, B.M., LEUNG, J.W.T., ROSENBERG, R.D., SMITH-BINDMAN, R., YANKASKAS, B.C. (2005):'Performance Benchmarks for Diagnostic Mammography', Radiology, **235**, pp. 775-790.

[3] BUADU, L.D., MURAKAMI, J., MURAYAMA, S., HASHIGUCHI, N., SAKAI, S., MASUDA, K., TOYOSHIMA, S., KUROKI, S., OHNO, S. (1999): 'Breast lesions: correlation of contrast medium enhancement patterns on MR images with histopathologic findings and tumor angiogenesis', Radiology, **200**, pp. 639-649

[4] KHUL, C.K., MIELCARECK, P., KLASCHIK, S., LEUTNER, C., WARDELMANN, E., GIESEKE, J., SCHILD, H.H. (1999): 'Dynamic breast MR imaging: are signal intensity time course data useful for differential diagnosis of enhancing lesions?', Radiology , **211**, pp. 101-110

[5] RANKIN, S.C (2000): 'MRI of the breast', The British journal of Radiology, **73**, pp. 806-818

[6] CHAN, T.F., VESE, L.A. (2001): 'Active Contours Without Edges', IEEE Trans. On Image Processing, **10(2)**, pp. 266-277

[7] OSHER, S., SETHIAN, J.A. (1988): 'Fronts Propagating with Curvature-Dependent Speed: Algorithms Based on Hamilton-lacobi Formulation', Journal of Computational Physics, **79**, pp. 12-49

ISSN: 1727-1983